

^{15}N CP/MAS NMR as a Tool for the Mechanistic Study of Mechanical Stimuli-Responsive Materials: Evidence for the Conformational Change of an Emissive Dimethylacridane Derivative

Toyotaka Nakae, Mineyuki Hattori,* and Yoshinori Yamanoi*

Cite This: *ACS Omega* 2023, 8, 12922–12927

Read Online

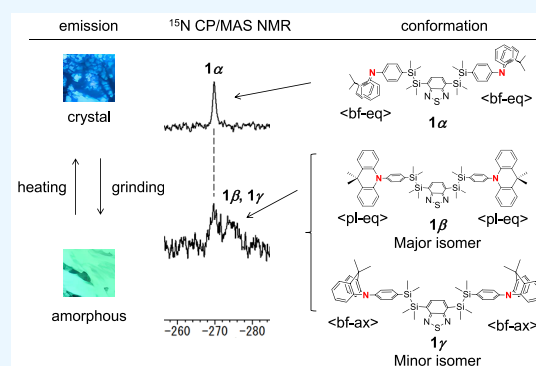
ACCESS |

Metrics & More

Article Recommendations

Supporting Information

ABSTRACT: Mechanochromic luminescent molecules are currently attracting considerable attention because of their promising technological applications, but understanding their mechanism of action is challenging and is thus hindering our deeper understanding of these materials. The conformational change of 9,9'-dimethyl-9,10-dihydroacridane derivative **1** was examined using solid-state ^{15}N nuclear magnetic resonance (NMR) spectroscopic techniques without using a specifically ^{15}N -labeled compound. A difference between the two conformers was clearly observed in the measurements and was assigned to the $\langle\text{pl}\rangle$ and $\langle\text{bf}\rangle$ spatial structures. The results were supported by quantum chemical calculations on ^{15}N NMR chemical shifts of each isomer. The technique presented here can clearly identify the structural changes caused by crushing a powder sample. Such structural changes are difficult to determine using X-ray diffraction (XRD) measurements.



1. INTRODUCTION

Stimuli-responsive crystalline molecules have attracted much interest over the past several years.¹ Among them, mechano-fluorochromic materials have made considerable progress in various intelligent responsive devices and security technologies.² There are many research examples of mechanochromic emission, but direct observation of structural variation before and after grinding a crystalline sample remains challenging. Most structural information on crystalline samples comes from single-crystal and/or powder X-ray diffraction studies, but these methods are insufficient to obtain structural information on amorphous samples, as such samples tend to show complex conformers. Thus, the investigation of structure–property relationships is key for rational molecular design to improve the performance of mechanochromic materials.

Solid-state NMR spectroscopy is increasingly employed to characterize solid-state functional materials,³ as it is a nondestructive characterization method suitable for complex materials and insoluble compounds. Many studies to date have focused on ^{13}C and ^{29}Si nuclei, whereas there have been limited measurements of ^{15}N nuclei.⁴ ^{15}N NMR spectroscopy is hampered by low sensitivity due to the very low natural abundance of ^{15}N (0.37%). The low nitrogen concentration in many molecules led researchers to believe that ^{15}N NMR investigations were impossible without ^{15}N enrichment. However, enrichment with ^{15}N is often not synthetically feasible. Thus, there are few reports of ^{15}N NMR measurements of mechanochromic materials.

We recently reported emissive organosilane crystalline compounds with nitrogen atoms in heterocyclic components.⁵ These compounds exhibit mechanochromic luminescence owing to a combination of the flexibility of the Si–Si bond and the conformational isomers of the cyclic *N*-arylamine.^{6,7} Among them, 4,7-bis(2-(4-(9,9-dimethylacridin-10(9*H*)-yl)-phenyl)-1,1,2,2-tetramethyldisilanyl)benzo[*c*][1,2,5]-thiadiazole adopts various conformational isomers **1α**, **1β**, and **1γ**, which contribute to changes in luminescence properties (Figure 1). The conformational structure in the crystalline state was found as **1α** studied by X-ray diffraction experiments. Grinding a crystalline sample with a mortar and pestle results in red-shifted emission. The morphology of the ground sample was amorphous, and no clear difference was observed in the solid-state ^{13}C NMR data between the crystalline and amorphous states in a preliminary study. Few investigations have focused on the isomeric conformational structure in the amorphous state of mechanochromic materials.⁸ In this study, we used solid-state ^{15}N NMR spectroscopy to identify structural modifications induced by the mechanochemical effect of grinding nitrogen-containing heterocycle **1** without

Received: January 6, 2023

Accepted: March 17, 2023

Published: March 30, 2023



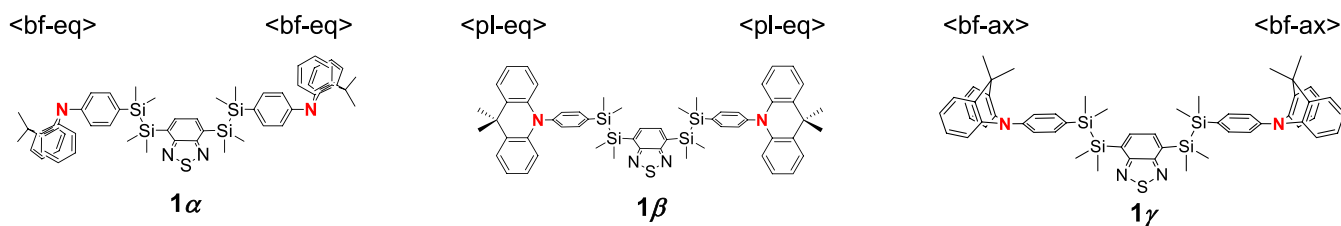


Figure 1. Possible conformational isomers **1α**, **1β** and **1γ** related to mechanochromic emission.

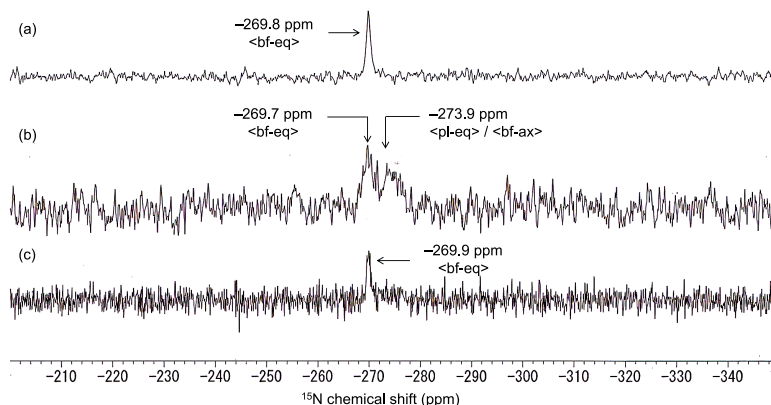


Figure 2. Solid-state ^{15}N NMR of **1** with reference to ^{15}N nitromethane as an external reference at rt. (a) Crystalline state. (b) Amorphous state with a grinding crystalline state. (c) After thermal annealing of the amorphous sample at 110 °C. LB = 0.

(partial) ^{15}N enrichment, and we present experimental and computational investigations of the relationship between the mechanochromic behavior and molecular structural changes of **1**.

2. RESULTS AND DISCUSSION

2.1. ^{15}N CP/MAS NMR Measurements. Compound **1** containing the 9,9'-dimethyl-9,10-dihydroacridane moiety possibly has quasi-equatorial (<eq>), quasi-axial (<ax>), butterfly (<bf>), and planar (<pl>) conformers. The <bf-eq> isomer is often observed in the crystalline state of the 9,9'-dimethyl-9,10-dihydroacridane structure, which shows a dihedral angle between the two phenyl groups in the 9,9'-dimethyl-9,10-dihydroacridane ring of about 30°. The structures of only a few <pl> isomers have been reported based on single-crystal X-ray structural analysis.¹⁰ Despite being far from common, ^{15}N NMR spectroscopy can provide useful information about the environment around N atoms, a key element in our material. The ^{15}N NMR spectrum of **1** in the crystalline state was measured to distinguish different classes and the connectivity of nitrogen in the molecule. The spectrum required the accumulation of 8,000 to 16,000 scans over a period of 24–48 h to obtain an adequate signal-to-noise ratio. The ^{15}N CP/MAS spectra of ^{15}N -unlabeled **1** are shown in Figure 2. A singlet signal was observed in the crystalline sample at -269.8 ppm relative to nitromethane. This signal can be assigned to the <bf-eq> conformer of 9,9'-dimethyl-9,10-dihydroacridane (Figure 2a) and is supported by single-crystal X-ray diffraction. The ^{15}N chemical shift of the benzothiadiazole group was observed at around -45 ppm (Figure S1a).¹¹ These observations were consistent with the presence of only one type of 9,9'-dimethyl-9,10-dihydroacridane group.

The grinding process induces a crystalline-to-amorphous phase transition, causing a change in the structure of the conformational isomers at the molecular level. Figure 2b shows the ^{15}N NMR spectrum for an amorphous sample of **1** after grinding and suggests the presence of multiple chemically distinct species. The peaks are located at -269.7 and -273.9 ppm, which indicates a different nitrogen environment of 9,9'-dimethyl-9,10-dihydroacridane in the ground sample compared with the unground sample.¹² We assigned the peak at lower magnetic field (-269.7 ppm) and at higher magnetic field (-273.9 ppm) to nitrogen atoms of <bf-eq> and another conformer, respectively, because the remaining peak at -269.7 ppm must be <bf-eq>. These results indicate that there is a chemical shift difference between the conformational isomers because the chemical shifts were affected by nitrogen nuclei in the molecule. The broadening of the peak in the amorphous state is presumably a result of random dipolar interaction in the amorphous state due to the deconstruction of CH– π intermolecular interactions with a lack of long-range periodicity. The ^{15}N chemical shift of the benzothiadiazole group did not change during the grinding process (Figure S1b).

Because of the flexible framework of **1**, the molecule can easily alter its conformational structure to effectively optimize intermolecular interactions. The two broad peaks disappear and the original single sharp peak at -269.9 ppm reappears after annealing at 100 °C (Figure 2c), indicating that the crystalline phase was recovered. This observation is consistent with the amorphous state returning to the crystalline state upon thermal stimulation. The ^{15}N CP/MAS NMR spectra indicate that the mechanochromic luminescence of **1** is relevant to molecular conformation and packing mode.

2.2. Theoretical Calculations. We calculated the energies of each conformational isomer of phenyl 9,9'-dimethyl-9,10-

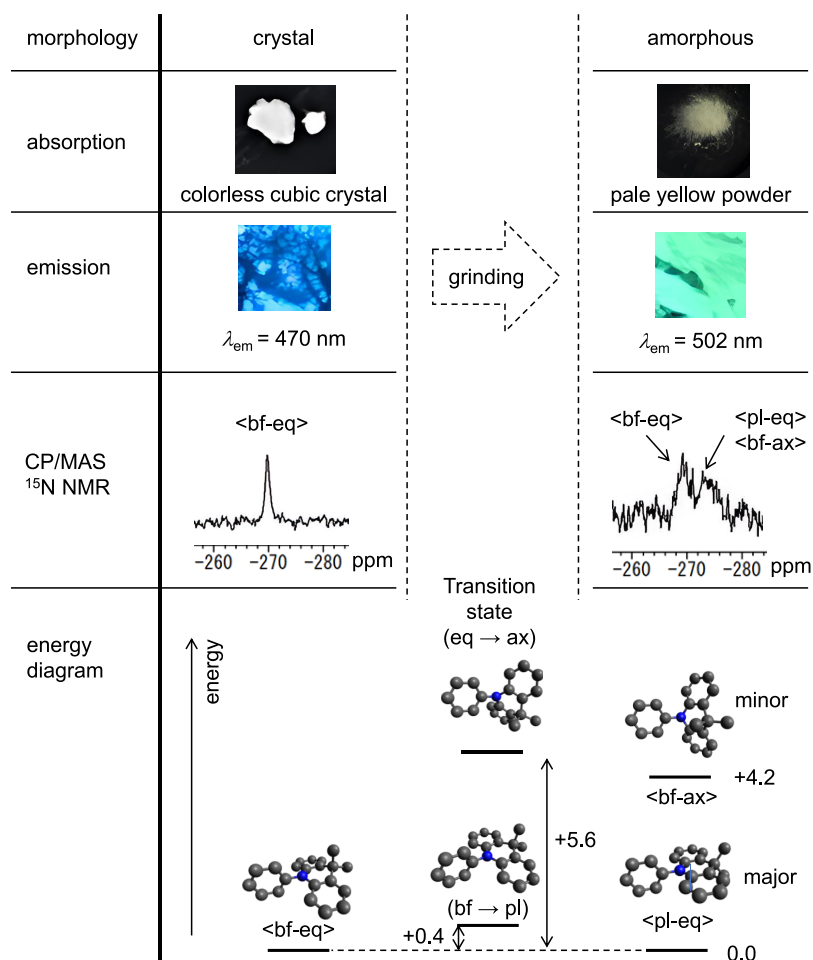


Figure 3. Structure–property relation. For simplicity, energy calculations were performed on phenyl 9,9'-dimethyl-9,10-dihydroacridane. The unit for numbers in the energy diagram is kcal/mol.

dihydroacridane to clarify its utility as a model compound. Possible conformational isomers and a proposed energy diagram are shown in Figure 3. The frequency analysis was performed on all optimized structures to ensure that the energy of the structure is the local minimum. Although $\langle\text{bf-eq}\rangle$ is the most stable isomer which is consistent with only one isomer observed in the crystal structure, studies performed on phenyl 9,9'-dimethyl-9,10-dihydroacridane revealed that the $\langle\text{bf}\rangle$ and $\langle\text{pl}\rangle$ conformations interconverted freely in the amorphous state with a low kinetic barrier ($\Delta G^\ddagger \approx 0.4$ kcal/mol) and no conformational energy difference ($\Delta E = 0.0$ kcal/mol). This result supported the theoretical possibility of coexisting populations of these conformations at rt. Therefore, when the crystalline sample is crushed under mechanical stress, $\langle\text{bf}\rangle$ and $\langle\text{pl}\rangle$ are present in equal amounts in the amorphous state at rt. The $\langle\text{bf-ax}\rangle$ conformer is also potentially present in the amorphous sample at a lower population due to the high internal energy ($\Delta G^\ddagger \approx 5.6$ kcal/mol). Therefore, the $\langle\text{bf-ax}\rangle$ conformer cannot be detected by NMR owing to the small amount present in the sample. The above results imply that **1** in the amorphous sample is a mixture of $\langle\text{bf-ax}\rangle$ and $\langle\text{pl-eq}\rangle$ at a ratio of $\sim 1:1$ and that grinding overcomes the transition energy for the internal conversion from $\langle\text{bf-eq}\rangle$ to $\langle\text{pl-eq}\rangle$ or $\langle\text{bf-ax}\rangle$. The calculation showed significant conformational flexibility and adoption of several conformers in the amorphous state.

Computational aspects of ^{15}N NMR shielding constants (chemical shifts) provide a powerful tool in structural studies of organic compounds.¹³ To verify the nitrogen assignments, ^{15}N NMR chemical shift calculations of phenyl 9,9'-dimethyl-9,10-dihydroacridane were performed based on the gauge including atomic orbital (GIAO) calculations using the Gaussian 16 program at the B3LYP/6-311+G** level of theory.¹⁴ The calculated results for each isomer are shown in the Supporting Information. The calculated ^{15}N NMR chemical shifts of $\langle\text{bf-eq}\rangle$, $\langle\text{pl-eq}\rangle$, and $\langle\text{ax-bf}\rangle$ were -259.5 , -264.1 , and -263.8 ppm relative to nitromethane, respectively.¹⁵ The comparison of $\langle\text{bf-eq}\rangle$ with $\langle\text{pl-eq}\rangle$ and $\langle\text{ax-bf}\rangle$ using ^{15}N NMR showed a high field shift of ~ 4 ppm, consistent with the results of ^{15}N NMR experimental measurements. The finding allows for a rationale for the mechanism of stimuli-responsive emission.

3. CONCLUSIONS

The present work investigated crystalline and amorphous samples of **1** using solid-state ^{15}N NMR and theoretical calculations. Because no spectroscopic evidence on conformational changes in the amorphous sample was presented, solid-state ^{15}N NMR complements X-ray diffraction studies on the conformations of nitrogen-containing heterocycles. The CP/MAS ^{15}N NMR data presented here provide more detailed structural information than previously reported ^{13}C CP/MAS

NMR studies. The ^{15}N NMR measurements indicate that a donor–acceptor–donor molecule of **1** after grinding exhibits at least two distinguishable environments around the N atoms between the ⟨bf⟩ and ⟨pl⟩ isomers with high conformational mobility. ^{15}N NMR chemical shifts were key to assigning the structures of the conformational forms and were sensitive to small changes in the local environment of the N atoms. The two different ^{15}N NMR peaks observed were derived from different nitrogen substitution patterns. The assignment was performed based on computational ^{15}N NMR studies for each isomer. ^{15}N NMR supported the fact that disruption and restoration of intermolecular CH– π interaction triggered by grinding and heating causes the conformational change of 9,9'-dimethyl-9,10-dihydroacridane, which are consistent with a previously proposed mechanism based on thermodynamic arguments. The energy levels of **1 α** , **1 β** , and **1 γ** are within 5.6 kcal/mol, and calculations suggest that **1** possesses significant conformational flexibility. Our work provides further evidence of a conformational change in **1** upon mechanical stimuli. Because ^{15}N NMR chemical shifts have a high regularity correlated to structure, they can be used as diagnostic indicators for identifying the structure of compounds in the solid state.

4. EXPERIMENTAL SECTION

4.1. Materials. All chemicals and reagents for CP/MAS ^{15}N NMR were obtained from commercial sources and used without additional purification. Compound **1** was prepared according to procedures previously reported by our group.^{6b}

4.2. Solid-State NMR Spectroscopy. The sample was packed into a 4 mm zirconia rotor and measured with ^{15}N cross-polarization/magic angle spinning (CP/MAS) NMR using a spectrometer (Bruker AVANCE III HD 600WB) at a Larmor frequency of 60.86 MHz. A Bruker MAS probe head (MAS4DR) was used with a HR-MAS rotor with 4 mm diameter (HZ05538) and a Teflon insert (50 μL), and the sample spin rate was 8 kHz. The amounts of crystalline and amorphous samples for ^{15}N CP/MAS NMR measurements were 38.37 and 29.92 mg, respectively. The ^{15}N chemical shifts were referenced to nitromethane at 0 ppm.¹⁶ NH_4Cl (10 atom % ^{15}N) was used as a second reference material, the NH_4 signal of which was set at -341.15 ppm. The samples were measured at ambient probe temperature.

4.3. Computational Details. The Gaussian 16 rev. C program was used to predict the ^{15}N NMR shielding constants of **1**. The geometries of all isomers of **1** were optimized at the B3LYP/6-31+G** level of theory, and the ^{15}N chemical shifts were calculated using the optimized structures by the gauge-independent atomic orbital method. The GIAO magnetic shielding tensor was -119.9 ppm for ^{15}N in nitromethane, and calculated ^{15}N NMR shifts were referenced to nitromethane.

■ ASSOCIATED CONTENT

SI Supporting Information

The Supporting Information is available free of charge at <https://pubs.acs.org/doi/10.1021/acsomega.3c00099>.

^{15}N NMR of **1**, and calculated data of nitromethane, ⟨bf-eq⟩, ⟨pl-eq⟩, and ⟨ax-bf⟩ of phenyl 9,9'-dimethyl-9,10-dihydroacridane (PDF)

■ AUTHOR INFORMATION

Corresponding Authors

Mineyuki Hattori – National Institute of Advanced Industrial Science and Technology (AIST), Tsukuba, Ibaraki 305-8565, Japan; orcid.org/0000-0002-0469-7146;

Email: mineyuki.hattori@aist.go.jp

Yoshinori Yamanoi – Department of Chemistry, School of Science, The University of Tokyo, Bunkyo-ku, Tokyo 113-0033, Japan; orcid.org/0000-0002-6155-2357;

Email: yamanoi@chem.s.u-tokyo.ac.jp

Author

Toyotaka Nakae – Department of Applied Chemistry, Tokyo Metropolitan University, Hachioji, Tokyo 192-0397, Japan;

orcid.org/0000-0002-3971-0611

Complete contact information is available at:

<https://pubs.acs.org/10.1021/acsomega.3c00099>

Notes

The authors declare no competing financial interest.

■ ACKNOWLEDGMENTS

This work was financially supported in part by the Nagase Science and Technology Foundation, the Tonen General Sekiyu Research/Development Encouragement & Scholarship Foundation, a Grant-in-Aid for Scientific Research (C) (No. JP22K05250), and Scientific Research on the Innovative Area “Soft Crystal: Science and Photofunctions of Flexible Response Systems with High Order” (Area 2903, No. JP17H06369) from the Ministry of Education, Culture, Sports, Science, and Technology, Japan. Solid-state NMR measurements were supported by the AIST Nanocharacterization Facility (ANCF) in the Advanced Research Infrastructure for Materials and Nanotechnology (No. JPMXP1222AT5021) sponsored by the Ministry of Education, Culture, Sports, Science, and Technology (MEXT), Japan.

■ REFERENCES

- (1) (a) Kato, M.; Ito, H.; Hasegawa, M.; Ishii, K. Soft Crystals: Flexible Response Systems with High Structural Order. *Chem. – Eur. J.* **2019**, *25*, 5105–5112. (b) Kato, M. Luminescent Platinum Complexes Having Sensing Functionalities. *Bull. Chem. Soc. Jpn.* **2007**, *80*, 287–294. (c) Sagara, Y.; Kato, T. Mechanically induced luminescence changes in molecular assemblies. *Nat. Chem.* **2009**, *1*, 605–610. (d) Møllerup, S. K.; Vang, S. Boron-based stimuli responsive materials. *Chem. Soc. Rev.* **2019**, *48*, 3537–3549. (e) Jobbágy, C.; Deák, A. Stimuli-Responsive Dynamic Gold Complexes. *Eur. J. Inorg. Chem.* **2014**, *2014*, 4434–4449. (f) Varughese, S. Non-covalent routes to tune the optical properties of molecular materials. *J. Mater. Chem. C* **2014**, *2*, 3499–3516. (g) Wang, X.-d.; Wolfbeis, O. S.; Meier, R. J. Luminescent probes and sensors for temperature. *Chem. Soc. Rev.* **2013**, *42*, 7834–7869. (h) Li, B.; Fan, H.-T.; Zang, S.-Q.; Li, H.-Y.; Wang, L.-Y. Metal-containing crystalline luminescent thermochromic materials. *Coord. Chem. Rev.* **2018**, *377*, 307–329.
- (2) (a) Zhao, J.; Chi, Z.; Zhang, Y.; Mao, Z.; Yang, Z.; Ubba, E.; Chi, Z. Recent progress in the mechanofluorochromism of cyanoethylene derivatives with aggregation-induced emission. *J. Mater. Chem. C* **2018**, *6*, 6327–6353. (b) Chi, Z.; Zhang, X.; Xu, B.; Zhou, X.; Ma, C.; Zhang, Y.; Liu, S.; Xu, J. Recent advances in organic mechanofluorochromic materials. *Chem. Soc. Rev.* **2012**, *41*, 3878–3896. (c) *Mechanochromic Fluorescent Materials: Phenomena, Materials and Applications*; Xu, J.; Chi, Z., Eds.; Royal Society of Chemistry: Cambridge, UK, 2014; Vol. 8. (d) Sagara, Y.; Yamane, S.; Mitani, M.; Weder, C.; Kato, T. Mechanoresponsive Luminescent Molecular

Assemblies: An Emerging Class of Materials. *Adv. Mater.* **2016**, *28*, 1073–1095. (e) Ito, S. Recent Advances in Mechanochromic Luminescence of Organic Crystalline Compounds. *Chem. Lett.* **2021**, *50*, 649–660.

(3) Molugu, T. R.; Lee, S.; Brown, M. Concepts and methods of solid-state NMR spectroscopy applied to biomembranes. *Chem. Rev.* **2017**, *117*, 12087–12132.

(4) For the representative examples, see: (a) Hayashi, S.; Hayamizu, K. Chemical Shift Standards in High-Resolution Solid-State NMR (^{15}N Nuclei). *Bull. Chem. Soc. Jpn.* **1991**, *64*, 688–690. (b) Munowitz, M.; Bachovchin, W. W.; Herzfeld, J.; Dobson, C. M.; Griffin, R. G. Acid-Base and Tautomeric Equilibria in the Solid State: ^{15}N NMR Spectroscopy of Histidine and Imidazole. *J. Am. Chem. Soc.* **1982**, *104*, 1192–1196. (c) Mason, J. Nitrogen Nuclear Magnetic Resonance Spectroscopy in Inorganic, Organometallic, and Bioinorganic Chemistry. *Chem. Rev.* **1981**, *81*, 205–227.

(5) For representative examples, see: (a) Nakae, M.; Nishio, M.; Yamanoi, Y. Photofunctional organosilicon compounds. *Bull. Jpn. Soc. Coord. Chem.* **2020**, *76*, 31–39. (b) Usuki, T.; Omoto, K.; Shimada, M.; Yamanoi, Y.; Kasai, H.; Nishibori, E.; Nishihara, H. Effects of substituents on the blue luminescence of disilane-linked donor-acceptor-donor triads. *Molecules* **2019**, *24*, 521. (c) Usuki, T.; Shimada, M.; Yamanoi, Y.; Ohto, T.; Tada, H.; Kasai, H.; Nishibori, E.; Nishihara, H. Aggregation-Induced Emission Enhancement from Disilane-Bridged Donor-Acceptor-Donor Luminogens Based on the Triarylamine Functionality. *ACS Appl. Mater. Interfaces* **2018**, *10*, 12164–12172. (d) Shimada, M.; Tsuchiya, M.; Sakamoto, R.; Yamanoi, Y.; Nishibori, E.; Sugimoto, K.; Nishihara, H. Bright Solid-State Emission of Disilane-Bridged Donor-Acceptor-Donor and Acceptor-Donor-Acceptor Chromophores. *Angew. Chem., Int. Ed.* **2016**, *55*, 3022–3026. (e) Shimada, M.; Yamanoi, Y.; Matsushita, T.; Kondo, T.; Nishibori, E.; Hatakeyama, A.; Sugimoto, K.; Nishihara, H. Optical Properties of Disilane-Bridged Donor-Acceptor Architectures: Strong Effect of Substituents on Fluorescence and Nonlinear Optical Properties. *J. Am. Chem. Soc.* **2015**, *137*, 1024–1027. (f) Nakae, T.; Miyabe, H.; Nishio, M.; Yamada, T.; Yamanoi, Y. Synthesis, structure and photophysical properties of yellow-green and blue photoluminescent dinuclear and octanuclear copper(I) iodide complexes with a disilanylene-bridged bispyridine ligand. *Molecules* **2021**, *26*, 6852. (g) Shimada, M.; Yamanoi, Y.; Ohto, T.; Pham, S.-T.; Yamada, R.; Tada, H.; Omoto, K.; Tashiro, S.; Shionoya, M.; Hattori, M.; Jimura, K.; Hayashi, S.; Koike, H.; Iwamura, M.; Nozaki, K.; Nishihara, H. Multifunctional Octamethyltetrasila[2.2]cyclophanes: Conformational Variations, Circularly Polarized Luminescence, and Organic Electroluminescence. *J. Am. Chem. Soc.* **2017**, *139*, 11214–11221.

(6) (a) Nakae, T.; Nishio, M.; Usuki, T.; Ikeya, M.; Nishimoto, C.; Ito, S.; Nishihara, H.; Hattori, M.; Hayashi, S.; Yamada, T.; Yamanoi, Y. Luminescent behavior elucidation of disilane-bridged D–A–D triad composed of phenothiazine and thienopyrazine. *Angew. Chem., Int. Ed.* **2021**, *60*, 22871–22878. (b) Miyabe, H.; Ujita, M.; Nishio, M.; Nakae, T.; Usuki, T.; Ikeya, M.; Nishimoto, C.; Ito, S.; Hattori, M.; Takeya, S.; Hayashi, S.; Saito, D.; Kato, M.; Nishihara, H.; Yamada, T.; Yamanoi, Y. A Series of D–A–D Structured Disilane-Bridged Triads: Structure and Stimuli-Responsive Luminescence Studies. *J. Org. Chem.* **2022**, *87*, 8928–8938.

(7) For other examples on conformational isomers of *N*-aryl cyclic amines, see: (a) Okazaki, M.; Takeda, Y.; Data, P.; Pander, P.; Higginbotham, H.; Monkman, A. P.; Minakata, S. Thermally activated delayed fluorescent phenothiazine–dibenzo[a,j]phenazine–phenothiazine triads exhibiting tricolor-changing mechanochromic luminescence. *Chem. Sci.* **2017**, *8*, 2677–2686. (b) Takeda, Y.; Data, P.; Minakata, S. Alchemy of donor–acceptor–donor multiphotofunctional organic materials: from construction of electron-deficient azaaromatics to exploration of functions. *Chem. Commun.* **2020**, *56*, 8884–8894. (c) Tanaka, H.; Shizu, K.; Nakanotani, H.; Adachi, C. Dual Intramolecular Charge-Transfer Fluorescence Derived from a Phenothiazine-Triphenyltriazine Derivative. *J. Phys. Chem. C* **2014**, *118*, 15985–15994. (d) Etherington, M. K.;

Franchello, F.; Gibson, J.; Northey, T.; Santos, J.; Ward, J. S.; Higginbotham, H. F.; Data, P.; Kurowska, A.; Santos, P. L. D.; Graves, D. R.; Batsanov, A. S.; Dias, F. B.; Bryce, M. R.; Penfold, T. J.; Monkman, A. P. Regio- and conformational isomerization critical to design of efficient thermally-activated delayed fluorescence emitters. *Nat. Commun.* **2017**, *8*, No. 14987. (e) Data, P.; Okazaki, M.; Minakata, S.; Takeda, Y. Thermally activated delayed fluorescence vs. room temperature phosphorescence by conformation control of organic single molecules. *J. Mater. Chem. C* **2019**, *7*, 6616–6621. (f) Takeda, Y.; Mizuno, H.; Okada, Y.; Okazaki, M.; Minakata, S.; Penfold, T.; Fukuhara, G. Hydrostatic Pressure – Controlled Ratiometric Luminescence Responses of Dibenzo[a,j]phenazine – Cored Mechanoluminophore. *ChemPhotoChem* **2019**, *3*, 1203–1211.

(8) For representative examples on mechanochromism investigated by ^{13}C or ^{31}P CP/MAS NMR, see: (a) Sheth, A. R.; Lubach, J. W.; Munson, E. J.; Muller, F. X.; Grant, D. J. W. Mechanochromism of Piroxicam Accompanied by Intermolecular Proton Transfer Probed by Spectroscopic Methods and Solid-Phase Changes. *J. Am. Chem. Soc.* **2005**, *127*, 6641–6651. (b) Utrera-Melero, R.; Huitorel, B.; Cordier, M.; Mevellec, J.-Y.; Massuyeau, F.; Latouche, C.; Martineau-Corcus, C.; Perruchas, S. Combining Theory and Experiment to Get Insight into the Amorphous Phase of Luminescent Mechanochromic Copper Iodide Clusters. *Inorg. Chem.* **2020**, *59*, 13607–13620.

(9) For example, see: (a) Lv, X.; Cao, X.; Wu, H.; Lin, H.; Ni, F.; Huang, H.; Zou, Y.; Yang, C. Realize efficient organic after glow from simple halogenated acridan derivatives. *Chem. Eng. J.* **2021**, *419*, No. 129598. (b) Han, M.; Xu, Z.; Lu, J.; Xie, Y.; Li, Q.; Li, Z. Intramolecular-locked triphenylamine derivatives with adjustable room temperature phosphorescence properties by the substituent effect. *Mater. Chem. Front.* **2021**, *6*, 33–39.

(10) (a) Hladka, I.; Volyniuk, D.; Bezikonny, O.; Kinzhybalov, V.; Bednarchuk, T. J.; Danyliv, Y.; Lytvyn, R.; Lazauskas, A.; Grazulevicius, J. V. Polymorphism of derivatives of *tert*-butyl substituted acridan and perfluorobiphenyl as sky-blue OLED emitters exhibiting aggregation induced thermally activated delayed fluorescence. *J. Mater. Chem. C* **2018**, *6*, 13179–13189. (b) Zheng, K.; Ni, F.; Chen, Z.; Zhong, C.; Yang, C. Polymorph-Dependent Thermally Activated Delayed Fluorescence Emitters: Understanding TADF from a Perspective of Aggregation State. *Angew. Chem., Int. Ed.* **2020**, *59*, 9972–9976. (c) Lin, T. A.; Chatterjee, T.; Tsai, W.-L.; Lee, W.-K.; Wu, M.-J.; Jiao, M.; Pan, K.-C.; Yi, C.-L.; Chung, C.-L.; Wong, K.-T.; Wu, C.-C. Sky-Blue Organic Light Emitting Diode with 37% External Quantum Efficiency Using Thermally Activated Delayed Fluorescence from Spiroacridine-Triazine Hybrid. *Adv. Mater.* **2016**, *28*, 6976–6983. (d) Liang, D.; Chen, X.-L.; Liao, J.-Z.; Hu, J.-Y.; Jia, J.-H.; Lu, C.-Z. Highly Efficient Cuprous Complexes with Thermally Activated Delayed Fluorescence for Solution-Processed Organic Light-Emitting Devices. *Inorg. Chem.* **2016**, *55*, 7467–7475. (e) Keruckiene, R.; Guzauskas, M.; Narbutaitis, E.; Tsiko, U.; Volyniuk, D.; Lee, P.-H.; Chen, C.-H.; Chiu, T.-L.; Lin, C.-F.; Lee, J.-H.; Grazulevicius, J. V. Exciplex-forming derivatives of 2,7-di-*tert*-butyl-9,9-dimethylacridan and benzotrifluoride for efficient OLEDs. *Org. Electron.* **2020**, *78*, No. 105576. (f) Fecková, M.; Kalis, I. K.; Roisnel, T.; Poul, P.; Pytela, O.; Klikar, M.; Guen, F. R.; Bureš, F.; Fakis, M.; Achelle, S. Photophysics of 9,9-Dimethylacridan-Substituted Phenylstyrylpyrimidines Exhibiting Long-Lived Intramolecular Charge-Transfer Fluorescence and Aggregation-Induced Emission Characteristics. *Chem. – Eur. J.* **2021**, *27*, 1145–1159.

(11) Yavari, I.; Botto, R. E.; Roberts, J. D. Nitrogen-15 nuclear resonance spectroscopy. Furazans and related systems. *J. Org. Chem.* **1978**, *43*, 2542–2544.

(12) Levy, G. C.; Lichter, R. L. *Nitrogen-15 Nuclear Magnetic Resonance Spectroscopy*; John Wiley & Sons: New York, 1979.

(13) *Encyclopedia of NMR*; Grant, D. M.; Harris, R. K., Eds.; Wiley: Chichester, 1996.

(14) For example, see: (a) Wolinski, K.; James, V.; Hinton, F.; Pulay, P. Efficient Implementation of the Gauge-Independent Atomic Orbital Method for NMR Chemical Shift Calculations. *J. Am. Chem. Soc.* **1990**, *112*, 8251–8260. (b) Ditchfield, R. Self-consistent

perturbation theory of diamagnetism I. A gauge-invariant LCAO method for N.M.R. chemical shifts. *Mol. Phys.* **1974**, *27*, 789–807.

(15) Calculated ^{15}N absolute shielding tensors (σ) were converted into ^{15}N NMR chemical shifts (δ) using the equation: $\delta = (\sigma_{\text{CH}_3\text{NO}_2} - \sigma)/(1 - 10^{-6}\sigma_{\text{CH}_3\text{NO}_2})$, where $\sigma_{\text{CH}_3\text{NO}_2}$ and σ are the ^{15}N NMR isotopic absolute shielding tensors of nitromethane and samples, respectively. Both values must be calculated at the same level of theory and with the same basis sets. See: (a) Samultsev, D. O.; Semenov, V. A.; Krivdin, L. B. On the accuracy factors and computational cost of the GIAO–DFT calculation of ^{15}N NMR chemical shifts of amides. *Magn. Reson. Chem.* **2017**, *55*, 1015–1021. (b) Samultsev, D. O.; Semenov, V. A.; Krivdin, L. B. On the accuracy of the GIAO-DFT calculation of ^{15}N NMR chemical shifts of the nitrogen-containing heterocycles—a gateway to better agreement with experiment at lower computational cost. *Magn. Reson. Chem.* **2014**, *52*, 222–230.

(16) (a) Ueda, T.; Nagatomo, S.; Masui, H.; Nakamura, N.; Hayashi, S. Hydrogen Bonds in Crystalline Imidazoles Studied by ^{15}N NMR and ab initio MO Calculations. *Z. Naturforsch. A* **1999**, *54*, 437–442. (b) Bertani, P.; Raya, J.; Bechinger, B. ^{15}N chemical shift referencing in solid state NMR. *Solid State Nucl. Magn. Reson.* **2014**, *61–62*, 15–18.